

Strong gravitational lensing — A probe for extra dimensions and Kalb-Ramond field

Sumanta Chakraborty ^{*} and Soumitra SenGupta [†]

Department of Theoretical Physics

Indian Association for the Cultivation of Science, Kolkata-700032, India

May 18, 2022

Abstract

Strong field gravitational lensing in the context of both higher spacetime dimensions and in presence of Kalb-Ramond field have been studied. After developing proper analytical tools to analyze the problem we consider gravitational lensing in three distinct black hole spacetimes — (a) four dimensional black hole in presence of Kalb-Ramond field, (b) brane world black holes with Kalb-Ramond field and finally (c) black hole solution in $f(T)$ gravity. In all the three situations we have depicted the behavior of three observables: the asymptotic position approached by the relativistic images, the angular separation and magnitude difference between the outermost images with others packed inner ones, both numerically and analytically. Difference between these scenarios have also been discussed along with possible observational signatures.

1 Introduction

Gravitational lensing is one of the most routinely used astrophysical observations to infer gravitational mass of distant galaxies or galaxy clusters. In broad sense, gravitational lensing corresponds to deflection of electromagnetic waves from its original trajectory á la spacetime curvature. Since spacetime curvature depends on the gravitational mass of the body producing it, the measurement of the deflection angle of the electromagnetic wave will be related to the mass of the gravitating object. Actually, gravitational lensing or more commonly known as the bending of light, in the context of solar system was used as the first observational verification of Einstein's general relativity. However all the situations depicted above correspond to weak field limit, where the spacetime curvature experienced by the electromagnetic wave is small such that the deflection angle is much small compared to 2π (see e.g., [1–3] and the references therein).

On the other hand, there can be situations where the deflection angle can become pretty large, e.g., when an electromagnetic wave passes close to a black hole, it can actually hover around the hole in closed loops before actually escaping it. In particular, there exist a sphere across the black hole, known as the photon sphere, where the deflection angle will even diverge. The strong field lensing develops an infinite

^{*}sumantac.physics@gmail.com; tpsc@iacs.res.in

[†]tpssg@iacs.res.in

set of discrete images near the central massive object, known as relativistic images, which has no analogue in the context of weak gravitational lensing. The analytical formulation of the strong gravitational lensing essentially started from the seminal work of Virbhadra and Ellis, where existence of such relativistic images were predicted in the context of Schwarzschild spacetime [4]. Immediately afterwards the concepts laid down in [4] were formulated in a more rigorous way by properly defining the strong field limit and providing better analytical understanding of the problem [5,6]. Subsequently it has been further generalized by providing the analytical framework in a general spherically symmetric spacetime [7] and has been applied to various black hole spacetimes which includes — Reissner-Nordström [8], Kerr [9,10], Einstein-Born-Infeld [11], Horava-Lifshitz [12], Brane world scenarios [13], dilaton [14–16], phantom [17,18] and Galileon [19]. It has also been applied to wormholes [20], regular black holes [21], self-dual black holes in loop quantum gravity [22] and naked singular spacetimes [23,24]. Also see [25–27] for recent reviews.

The growing interest in the strong gravitational lensing is mainly due to the reason that one can use the lensing phenomenon to infer properties about the regions in the vicinity of the black hole horizon. In particular through gravitational lensing one can infer the region of black hole spacetime, known as black hole shadows. Current observations cannot access these shadows mainly due to low resolution, but in upcoming years with event horizon telescope, very long baseline interferometry, square kilometer array one would be able to resolve regions very near the black hole where the strong field gravitational lensing will become very important [28–33].

Given the current theoretical importance and future observational backdrops it is important to study some fundamental physics using strong gravitational lensing. Two such important aspects are presence of extra spacetime dimensions and Kalb-Ramond field or spacetime torsion. In the higher dimensional physics the standard scenario corresponds to matter fields confined to the brane, while gravity can exist in the bulk. In string theoretic description there exists a closed string excitation leading to a second rank antisymmetric tensor, known as the Kalb-Ramond field. Thus if the Kalb-Ramond field exists then it must invade the extra dimensions [34], suggesting that one has to employ the Gauss-Codazzi formalism to obtain the effective theory on the four dimensional hypersurface [35–38]. This antisymmetric tensor plays an important role in many areas of physics, which includes, e.g., theories of gravity formulated using twistors requires the Kalb-Ramond field [39], spacetime with Kalb-Ramond field can become optically active [40], Kalb-Ramond field can give rise to topological defects, which might lead to intrinsic angular momentum to the structures in our galaxies [41], Kalb-Ramond field also plays an important role in understanding leptogenesis [42], Kalb-Ramond field also affects the anisotropy in cosmic microwave background [43] and so on. In particular given the second rank antisymmetric Kalb-Ramond field one can construct a third rank antisymmetric tensor, which appears naturally in the gravity theory and can act as the missing part of general relativity, the spacetime torsion [44]. However in this work we will *not* identify spacetime torsion as originating from the Kalb-Ramond field, but shall treat them on distinct footing. With Kalb-Ramond field we will discuss two situations — (i) Kalb-Ramond field in four spacetime dimensions and (ii) Kalb-Ramond field exists in higher dimensions (referred to as the bulk) and its effect on a lower dimensional hypersurface (known as the brane). Then we separately discuss the scenario with spacetime torsion in the context of $f(T)$ gravity, which has interesting cosmological implications [45–51]. In this work we derive the gravitational lens equation and the corresponding observables have been derived in the context of Kalb-Ramond field in four and in higher spacetime dimensions as well as in the presence of spacetime torsion in the form of $f(T)$ gravity.

The paper is organized as follows: In [Section 2](#) we present necessary analytical results in a compact manner for the most general static, spherically symmetric solution. The same is subsequently applied in [Section 3](#) to three different situations — (a) Kalb-Ramond field in four spacetime dimensions (discussed in [Section 3.1](#)), (b) Kalb-Ramond field in higher dimensions (illustrated in [Section 3.2](#)) and finally (c)

spacetime torsion in the context of $f(T)$ gravity (depicted in [Section 3.3](#)). We end with a discussion on the results obtained. Detailed calculations are presented in [Appendix A](#).

2 Strong gravitational lensing: Analytical results

Static and spherically symmetric spacetimes form an integral part of black hole physics where all the basic features of black holes can be demonstrated and can be used to understand and generalize the techniques for more general scenarios. In this work as well, we will content ourselves with static and spherically symmetric spacetimes but in the presence of Kalb-Ramond field and extra dimensions. We will first summarize the key concepts involved and the observables related to strong gravitational lensing for a general static, spherically symmetric spacetime before considering the spacetimes of our interest.

For this purpose, let us start with a static, spherically symmetric spacetime described by the following line element,

$$ds^2 = -f(r)dt^2 + \frac{dr^2}{g(r)} + r^2 d\Omega_2^2 \quad (1)$$

where, $f(r)$ and $g(r)$ are arbitrary functions of the radial coordinate with $d\Omega_2^2$ being the line element on two sphere. (Some interesting features regarding this line element have been explored in [\[52–55\]](#)) We further assume that the spacetime is asymptotically flat, i.e., $f(r \rightarrow \infty) = 1$ and $g(r \rightarrow \infty) = 1$. We will be exclusively considering the trajectories of photons in this work and the single most important radius associated with those trajectories correspond to the radius of photon circular orbit r_{ph} . This can be obtained by solving the following equation,

$$rf'(r) - 2f(r) = 0 \quad (2)$$

where $f'(r)$ stands for derivative of the metric function $f(r)$ with respect to radial coordinate. Note that the above equation is independent of the structure of $g(r)$, i.e., the g_{tt} component is solely responsible for the structure of photon sphere. The trajectory of a photon is specified by two constants of motion, the energy E and the angular momentum L . In terms of these two constants of motion the trajectory of the photon can be represented by the following differential equation,

$$\frac{d\phi}{dr} = \frac{L}{r^2} \sqrt{\frac{f}{g} \left[E^2 - f(r) \frac{L^2}{r^2} \right]}^{-1/2} \quad (3)$$

The minimum radius r_0 that a photon can travel with energy E and angular momentum L corresponds to the one when value of the term inside square root vanishes. Thus the impact parameter $b = L/E$ can be written in terms of r_0 as, $(1/b^2) = (f(r_0)/r_0^2)$ (see [Fig. 1](#) for details). Hence the orbit equation gets modified to,

$$\frac{d\phi}{dr} = \frac{1}{r^2} \sqrt{\frac{f}{g} \left[\frac{f(r_0)}{r_0^2} - \frac{f(r)}{r^2} \right]}^{-1/2} \quad (4)$$

Integrating this orbit equation one obtains the deflection angle suffered by the photon as it travels from

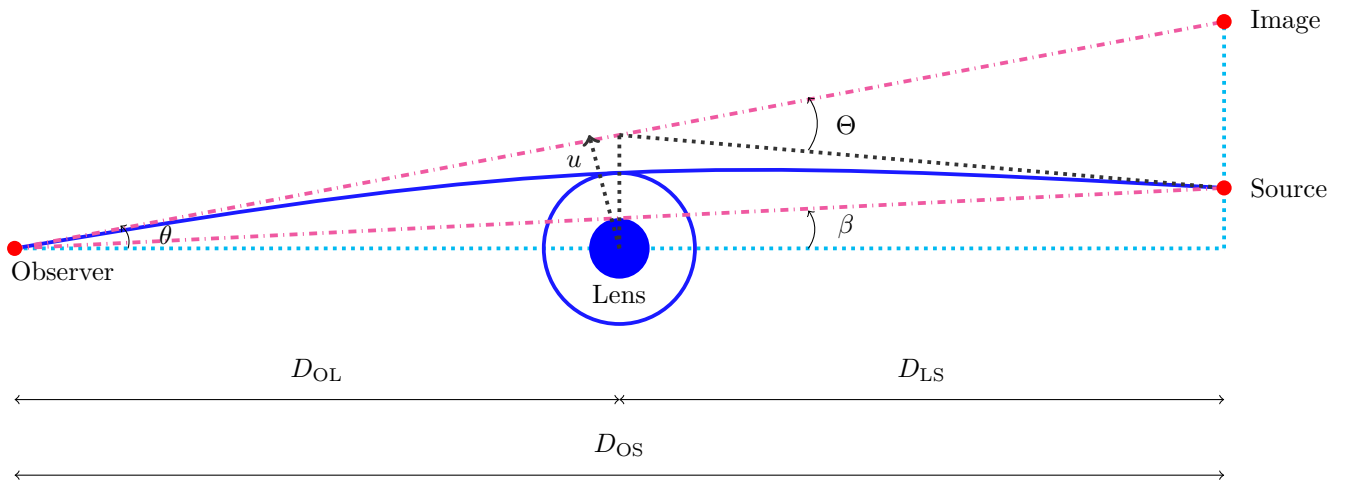


Figure 1: Schematic diagram of strong gravitational lensing. The observer, the source, the lens and the image are depicted. The light emitted by the source (thick blue line) gets deflected by the lens and reaches the observer. From the viewpoint of the observer it will appear that the light ray is originating from the image. Three different angular separations are also shown, β being the angular separation between the source and the lens, θ stands for the angular difference between the image and the lens while Θ representing the deflection. Three distances D_{OL} , D_{LS} and D_{OS} representing the observer-lens, lens-source and observer-source have also been shown.

asymptotic infinity to the impact distance r_0 as,

$$\Theta = -\pi + \int_{x_0}^{x_\infty} dx R(x, r_0) F(x, r_0); \quad R(x, r_0) = 2 \frac{dr}{dx} \sqrt{\frac{f}{g} \frac{r_0}{r^2}}; \quad F(x, r_0) = \left[f(r_0) - \frac{r_0^2}{r^2} f(r) \right]^{-1/2} \quad (5)$$

In the above integral we have introduced a new variable $x = x(r)$, yet unspecified, such that $x(r_0) = x_0$ and $x(\infty) = x_\infty$. A standard choice is to assume $x = (f(r) - f(r_0))/(1 - f(r_0))$, such that as $r \rightarrow \infty$ one obtains $x_\infty = 1$, while for $r \rightarrow r_0$ one arrives at $x_0 = 0$. However we will not assume any such particular expression for x and will keep it general for the moment, only with $x_0 = 0$. The reason for separating out the integral in the deflection angle into two parts is immediate, while $R(x, r_0)$ is finite for all values of r , the other term $F(r_0, x)$ diverges as the photon approaches $r = r_0$. To deal with the divergence, one can Taylor expand the function $f(r_0) - (r_0^2 f(r)/r^2)$ inside the inverse square root around $r = r_0$. This essentially implies expansion around $x = 0$. Performing the expansion, one can separate out the integral into a regular part and a divergent part. The divergent part can be integrated analytically and expanded around $r = r_{\text{ph}}$ (see [Appendix A](#) for detailed derivation).

Further one can introduce another variable $u = r/\sqrt{f(r)}$ as a substitute for the radial coordinate r , such that u_0 leads to the impact parameter of the photon. Then rewriting the divergent integral in terms of the new variable u , we finally obtain the lens equation to read,

$$\Theta(\theta) = -\bar{a} \ln \left(\frac{\theta D_{\text{OL}}}{u_{\text{ph}}} - 1 \right) + \bar{b} \quad (6)$$

where, D_{OL} stands for the distance between the observer and the lens, θ being the angle between the image and the lens and $u_{\text{ph}} = r_{\text{ph}}/\sqrt{f(r_{\text{ph}})}$. The other objects appearing in the above expression has the following structure in terms of the functions $f(r)$, $g(r)$ and their derivatives,

$$\bar{a} = \sqrt{\frac{2f(r_{\text{ph}})}{g(r_{\text{ph}}) \left[-r_{\text{ph}}^2 f''(r_{\text{ph}}) + 2f(r_{\text{ph}}) \right]}} \quad (7)$$

$$\bar{b} = -\pi + b_{\text{R}} + \bar{a} \ln \left(\frac{\left[-r_{\text{ph}}^2 f''(r_{\text{ph}}) + 2f(r_{\text{ph}}) \right] \left[1 - f(r_{\text{ph}}) \right]^2}{r_{\text{ph}}^2 f(r_{\text{ph}}) \left[f'(r_{\text{ph}}) \right]^2} \right) \quad (8)$$

$$b_{\text{R}} = \int_0^1 dx \left\{ \frac{2r_{\text{ph}}}{r(x)^2} \sqrt{\frac{f(x)}{g(x)}} \left(\frac{1 - f(x)}{f'(x)} \right) \left[f(r_{\text{ph}}) - \frac{r_{\text{ph}}^2}{r(x)^2} f(x) \right]^{-1/2} - \frac{2\bar{a}}{x} \right\} \quad (9)$$

where, we have used the standard expression connecting x and r to be, $x = (f(r) - f(r_{\text{ph}}))/(1 - f(r_{\text{ph}}))$. With all these identifications [Eq. \(6\)](#) yields the general lens equation for gravitational lensing in the strong field regime. The corresponding observables are — (i) the deflection angle θ_∞ corresponding to the outermost image, (ii) the angular separation s between the outermost image and the inner ones and finally (iii) the astronomical magnitude difference r between the outermost image and the inner images. These

three observables are expressed in terms of the variables introduced above as,

$$\theta_\infty = \frac{u_{\text{ph}}}{D_{\text{OL}}}, \quad (10)$$

$$s = \theta_\infty \exp\left(\frac{\bar{b}}{\bar{a}} - \frac{2\pi}{\bar{a}}\right) \quad (11)$$

$$r = \frac{5\pi}{\bar{a} \log 10} \quad (12)$$

Thus there is a one to one mapping between the observables (θ_∞, s, r) and the parameters of the model, namely, $(u_{\text{ph}}, \bar{a}, \bar{b})$. Hence given the metric functions $f(r)$ and $g(r)$ one can compute the photon radius and hence each terms in the Lens equation. Then one can numerically compute the observables and study their difference with the corresponding Schwarzschild one as well as the behavior of these observables as the corresponding parameters in the gravitational field are modified. This is what we will do next for three black hole spacetime in presence of Kalb-Ramond field. It is convenient to choose $GM = 1$ along with $c = 1$ and we will write the respective expressions accordingly.

3 Lensing in presence of Kalb-Ramond field and extra dimensions

In this section, we will discuss three situations involving Kalb-Ramond field as well as extra spatial dimensions. In the first example, we mainly concentrate on the effect of Kalb-Ramond field in four dimensional static spherically symmetric spacetimes and the resulting modifications of the strong gravitational lensing observables. Then we introduce additional spatial dimensions and their possible signatures in the effective four-dimensional spacetime. This, in addition to Kalb-Ramond field the effects originating from the bulk spacetime will also be addressed. Finally, we concentrate on a spherically symmetric and static solution in $f(T)$ theories of gravity. We will now elaborate on these different scenario.

3.1 Kalb-Ramond field in four spacetime dimensions and gravitational lensing

Let us consider a situation when the Kalb-Ramond field is present in four spacetime dimensions. The corresponding gravitational action would involve the Einstein-Hilbert term, i.e., the Ricci scalar and the term $\sqrt{-g}H_{abc}H^{abc}$, where H_{abc} is the Kalb-Ramond field. Our interest lies in the static, spherically symmetric solution with this particular modifications of the Einstein-Hilbert action. It will turn out that with these enhanced symmetries the Kalb-Ramond field has a single non-trivial spherically symmetric component, which to leading order behaves as, $(2/r^2)\sqrt{(b/24\pi G_N)}$ [56,57]. Thus the parameter b captures the existence of Kalb-Ramond field, since for $b = 0$, the Kalb-Ramond field identically vanishes. Solving the gravitational field equations, one obtains the following behaviour of the metric functions,

$$f(r) = 1 - \frac{2}{r} - \frac{b}{3r^3} \quad (13)$$

$$g(r) = 1 - \frac{2}{r} - \frac{b}{r^2} \quad (14)$$

where we have set $GM = 1$ as stated earlier [56]. Also note that if the Kalb-Ramond parameter b vanishes, the above metric elements reduces to that of Schwarzschild metric. Let us compute the observables

associated with gravitational lensing for this particular solution. The first and most important thing corresponds to the computation of the photon circular orbit, which can be obtained by solving the following algebraic equation,

$$r^3 - 3r^2 - \frac{5b}{6} = 0 \quad (15)$$

The corresponding solution is given in terms of the Kalb-Ramond parameter b as,

$$r_{\text{ph}} = \frac{\left(\sqrt{\left(\frac{5b}{3}\right)^2 + \frac{10b}{3} + 2}\right)^{1/3}}{\sqrt[3]{2}} + \frac{\sqrt[3]{2}}{\left(\sqrt{\left(\frac{5b}{3}\right)^2 + \frac{10b}{3} + 2}\right)^{1/3}} + 1 \quad (16)$$

The theoretical variables associated with this model are the impact parameter associated with the photon circular orbit, i.e., $u_{\text{ph}} = r_{\text{ph}}/\sqrt{f(r_{\text{ph}})}$ as well as the parameters \bar{a} and \bar{b} as mentioned in Eq. (8) and Eq. (9) respectively. The analytical expressions for these variables in terms of the Kalb-Ramond parameter b reads,

$$u_{\text{ph}} = \frac{r_{\text{ph}}^{5/2}}{\sqrt{r_{\text{ph}}^3 - 2r_{\text{ph}}^2 - \frac{b}{3}}} \quad (17)$$

$$\bar{a} = \left[\frac{r_{\text{ph}}^2 + \frac{b}{2}}{r_{\text{ph}}^2 - br_{\text{ph}} + \frac{5b}{6}}\right]^{1/2} \left[1 + \frac{5b}{3r_{\text{ph}}^3}\right]^{-1/2} \quad (18)$$

$$\bar{b} = -\pi + b_{\text{R}} + \bar{a} \ln \left(\frac{2 \left[r_{\text{ph}}^3 + \frac{5b}{3} \right] \left[\frac{r_{\text{ph}}^2 + \frac{b}{6}}{r_{\text{ph}}^2 + \frac{b}{2}} \right]^2}{r_{\text{ph}}^3 - 2r_{\text{ph}}^2 - \frac{b}{3}} \right) \quad (19)$$

Note that these three variables are sufficient to determine the three observables θ_{∞} , r and s , thanks to the relations presented in Eq. (10), Eq. (11) and Eq. (12) respectively. The additional information necessary to have a numerical estimate are the mass and distance of the central object. The best such candidate corresponds to the supermassive black hole Sgr A* with mass $M_{\bullet} = 4.31 \times 10^6 M_{\odot}$, where M_{\odot} is the mass of the sun and $D_{\text{OL}} = D_{\bullet} = 8.33$ kpc. The numerical estimates of the observables (θ_{∞}, s, r) and the theoretical parameters ($u_{\text{ph}}, \bar{a}, \bar{b}$) have been presented in Table 1 for various values of the Kalb-Ramond parameter b along with the corresponding Schwarzschild values for comparison.

As a final ingredient we present the explicit form of the lens equation for the four-dimensional Kalb-Ramond black hole, where to leading order in the Kalb-Ramond parameter b , the regular part of the integral in lens equation yield, $b_{\text{R}} = 0.9496 + 0.0528 b$. Hence the deflection angle becomes,

$$\Theta(\theta) = -2.192 + 0.0528 b + \left\{ \frac{r_{\text{ph}}^2 + \frac{b}{2}}{\left[1 + \frac{5b}{3r_{\text{ph}}^3}\right] \left(r_{\text{ph}}^2 - br_{\text{ph}} + \frac{5b}{6}\right)} \right\}^{1/2} \ln \left(\frac{2u_{\text{ph}} \left[r_{\text{ph}}^3 + \frac{5b}{3} \right] \left[\frac{r_{\text{ph}}^2 + \frac{b}{6}}{r_{\text{ph}}^2 + \frac{b}{2}} \right]^2}{\left(r_{\text{ph}}^3 - 2r_{\text{ph}}^2 - \frac{b}{3}\right) (\theta D_{\text{OL}} - u_{\text{ph}})} \right) \quad (20)$$

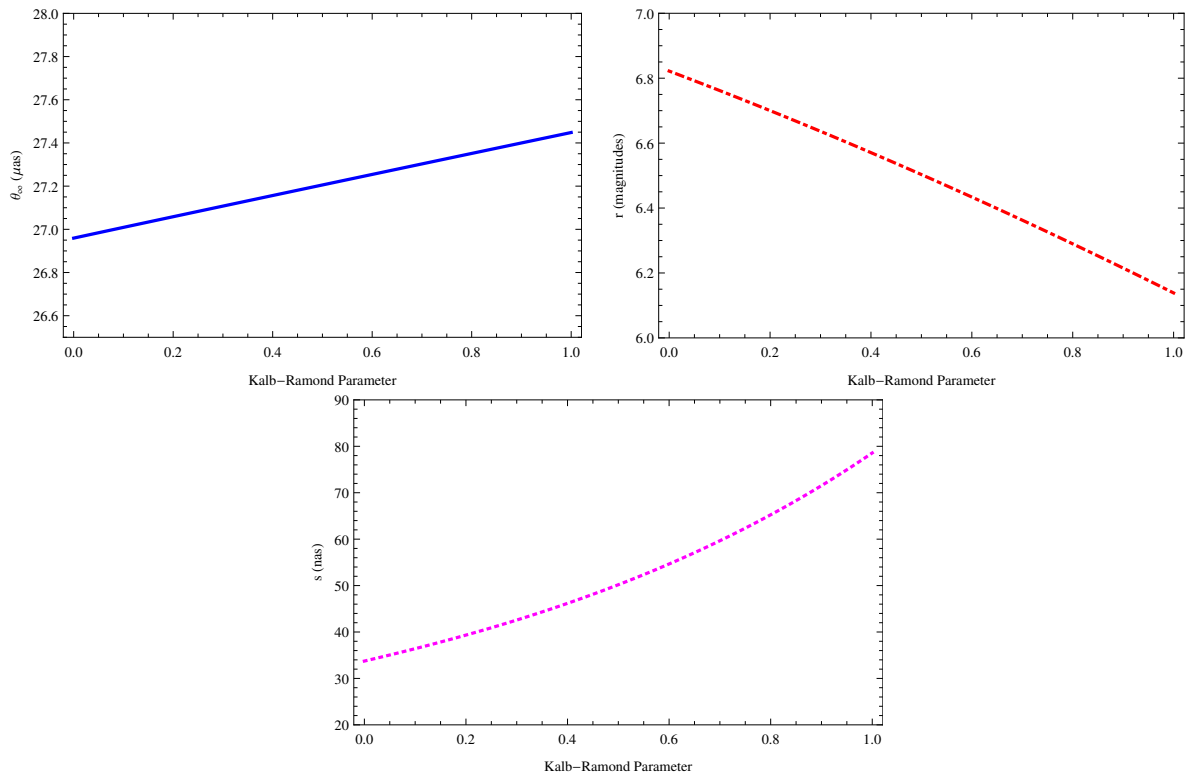


Figure 2: Variation of the three observables — (a) the deflection angle θ_∞ in micro-arcsecond, (b) the magnitude difference r between the outermost and inner images and finally (c) the angular difference between the outermost and inner images s in nano-arcsecond have been presented as the Kalb-Ramond parameter b increases. Hence in four spacetime dimensions as the Kalb-Ramond parameter increases the corresponding deflection angle and angular separation increases, while the magnitude difference exhibits an opposite effect. See text for more discussions.

Table 1: The observables associated with strong gravitational lensing, namely (θ_∞, s, r) and the theoretical parameters of the model, i.e., $(u_{\text{ph}}, \bar{a}, \bar{b})$ have been presented. Numerical estimates for both the Schwarzschild black hole and the black hole with Kalb-Ramond field for three possible Kalb-Ramond parameters are illustrated. In all these calculations, the central massive object is taken to be Sgr A^* with mass $M_\bullet = 4.31 \times 10^6 M_\odot$ and distance $D_{\text{OL}} = 8.33$ kpc, where M_\odot is the mass of the sun. Further, the angles θ_∞ and s are expressed in units of micro-arcsecond (μas), and nano-arcsecond (nas) respectively. All the distances are measured with $GM_\bullet/c^2 = 1$ unit.

Observables and Parameters	Schwarzschild	Torsion Coupled Hole		
		$b = 0.2$	$b = 0.5$	$b = 0.8$
θ_∞ (μas)	26.96	27.06	27.21	27.35
s (nas)	33.74	39.34	50.18	65.25
r (mag)	6.82	6.7	6.5	6.29
$u_{\text{ph}}(GM_\bullet/c^2)$	5.20	5.22	5.24	5.27
\bar{a}	1	1.02	1.05	1.08
\bar{b}	-0.40	-0.37	-0.32	-0.27

From both [Table 1](#) and [Fig. 2](#) one can understand the effect of Kalb-Ramond field on gravitational lensing both quantitatively and qualitatively. From [Fig. 2](#) it is clear that the angular deflection and angular separation increases monotonically as the Kalb-Ramond parameter is increased, while the magnification parameter depicts an exactly opposite behaviour. Similar features are also present in [Table 1](#), but according to the numerical estimates, both the angular deflection and angular separation are larger compared to the Schwarzschild value. For example, when $b = 0.5$, the deflection angle is almost one percent while the angular separation is 49 percent larger. On the other hand, the magnification is almost five percent less compared to the Schwarzschild counterpart.

3.2 Kalb-Ramond field and extra dimensions

Extra spatial dimensions are known to play crucial role in addressing the hierarchy problem. In some models of extra dimensions the matter fields are confined to the four-dimensional brane, while gravity extends over the higher dimensions. From stringy viewpoint the Kalb-Ramond field being a closed string mode like gravity, can also probe the extra spacetime dimensions. Hence in presence of both Kalb-Ramond field and extra dimensions it is important to consider the Kalb-Ramond field in the bulk spacetime. The natural question arising in this context is to address how the gravity looks like from a four-dimensional perspective in this scenario. This question has been answered recently in [\[58\]](#), where possible effects of higher dimensional Kalb-Ramond field in the context of brane world were studied. Further a static, spherically symmetric solution on the brane was also derived. In this section we consider strong gravitational lensing from a similar but slightly modified perspective.

There will be two modifications in the effective gravitational field equations on the brane — (a) effects of Kalb-Ramond field inherited from the bulk and (b) the effect of bulk Weyl tensor projected on the brane [\[58\]](#). The projected Kalb-Ramond field in presence of static and spherical symmetry is represented by a single function $h(r)$, which to the leading order behaves as $\sqrt{\tau/\kappa_5^2}(1/r^2)$, where κ_5 is the five-

dimensional gravitational constant and τ is the parameter characterizing the Kalb-Ramond field. With this solution for the Kalb-Ramond field the corresponding solution for the metric elements in the effective four dimensional spacetime on the brane becomes,

$$f(r) = 1 - \frac{2}{r} - \frac{a}{r^2} - \frac{2\tau}{r^3} \quad (21)$$

$$g(r) = 1 - \frac{2}{r} - \frac{a - \tau}{r^2} \quad (22)$$

where, $a = (3\alpha P_0/2)$ has been inherited from the bulk Weyl tensor, such that, $\alpha = (1/4\pi G_N \lambda_T)$ with λ_T being the brane tension and P_0 measures the effect of bulk Weyl tensor. Note that if the torsion parameter τ vanishes, the above solution reduces to the well known black hole solution on the brane derived in [59]. In this case the photon circular orbit can be obtained by solving the following algebraic equation,

$$r^3 - 3r^2 - 2ar - 5\tau = 0 \quad (23)$$

which can be solved to yield the photon radius as,

$$r_{\text{ph}} = 1 + \frac{2^{1/3}(9 + 6a)}{3 \left(54 + 54a + 135\tau + \sqrt{(54 + 54a + 135\tau)^2 - 4(9 + 6a)^3} \right)^{1/3}} + \frac{\left(54 + 54a + 135\tau + \sqrt{(54 + 54a + 135\tau)^2 - 4(9 + 6a)^3} \right)^{1/3}}{3 \times 2^{1/3}} \quad (24)$$

The other quantities of importance are the three theoretical parameters for this model — (a) the impact parameter at the photon radius, i.e., $u_{\text{ph}} = r_{\text{ph}}/\sqrt{f(r_{\text{ph}})}$, (b) the two parameters \bar{a} and \bar{b} associated the gravitational lens equation. These three parameters read as follows,

$$u_{\text{ph}} = \frac{r_{\text{ph}}^{5/2}}{\sqrt{r_{\text{ph}}^3 - 2r_{\text{ph}}^2 - ar_{\text{ph}} - 2\tau}} \quad (25)$$

$$\bar{a} = r_{\text{ph}} \sqrt{\frac{r_{\text{ph}}^3 - 2r_{\text{ph}}^2 - ar_{\text{ph}} - 2\tau}{(r_{\text{ph}}^3 + 2ar_{\text{ph}} + 10\tau)(r_{\text{ph}}^2 - 2r_{\text{ph}} + \tau - a)}} \quad (26)$$

$$\bar{b} = -\pi + b_R + \bar{a} \ln \left[\frac{(r_{\text{ph}}^3 + 2ar_{\text{ph}} + 10\tau)(2r_{\text{ph}}^2 + ar_{\text{ph}} + 2\tau)^2}{(r_{\text{ph}}^3 - 2r_{\text{ph}}^2 - ar_{\text{ph}} - 2\tau)(2r_{\text{ph}}^2 + 2ar_{\text{ph}} + 6\tau)} \right] \quad (27)$$

Then using Eq. (10), Eq. (11) and Eq. (12) we can determine the three observables θ_∞ , s and r respectively from the expressions of u_{ph} , \bar{a} and \bar{b} derived above. As in the previous section here also we use sgr A* as the black hole candidate with its mass and distance being quoted in the earlier section. The numerical estimates of the observables as well as the theoretical parameters are presented in Table 2 for various values of the Kalb-Ramond parameter τ and the bulk inherited parameter a . Corresponding values of the parameters and observables are also presented for Schwarzschild spacetime for direct comparison. Moreover, the variation of the observables θ_∞ , s and r with the Kalb-Ramond parameter τ are presented

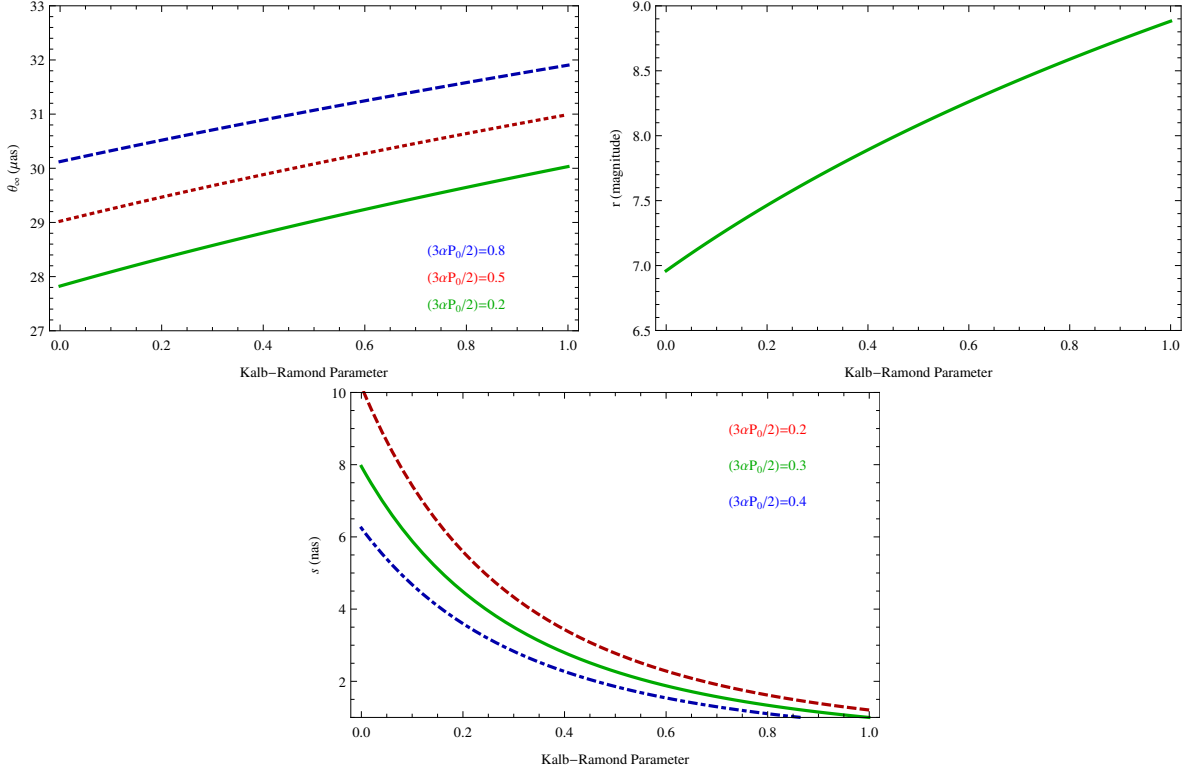


Figure 3: Variation of the three observables — (a) the deflection angle θ_∞ in micro-arcsecond, (b) the magnitude difference r between the outermost and inner images and finally (c) the angular difference between the outermost and inner images s in nano-arcsecond have been illustrated as the Kalb-Ramond parameter τ increases. It is clear that as the Kalb-Ramond parameter increases the corresponding deflection angle and magnitude difference increases, while the angular separation exhibits an opposite effect. See text for discussions.

Table 2: Numerical estimations of the lensing observables (θ_∞, s, r) and the parameters of the theory namely, $(u_{\text{ph}}, \bar{a}, \bar{b})$ have been provided. Results for the Schwarzschild black hole as well as the black hole in effective field theory for four possible choices of the higher dimensional Kalb-Ramond parameter τ and the bulk inherited parameter $a = 3\alpha P_0/2$ are presented. In all these calculations, the central black hole is assumed to be Sgr A^* having mass $M_\bullet = 4.31 \times 10^6 M_\odot$, which is $D_{\text{OL}} = 8.33$ kpc away. In addition, the angle θ_∞ and s are expressed in units of micro-arcsecond (μas) and nano-arcsecond (nas) respectively, for convenience. All the distances are presented in $GM_\bullet/c^2 = 1$ unit.

Observables and Parameters	Schwarzschild	In Effective Theory			
		$b = 0.2$ $a = 0$	$b = 0.7$ $a = 0.3$	$b = 0$ $a = 0.4$	$b = 0.9$ $a = 0.4$
θ_∞ (μas)	26.96	27.53	29.79	28.63	30.50
s (nas)	33.74	8.75	1.57	6.24	0.95
r (mag)	6.82	7.39	8.43	7.08	8.72
$u_{\text{ph}}(GM_\bullet/c^2)$	5.20	5.31	5.74	5.52	5.89
\bar{a}	1	0.92	0.81	0.96	0.78
\bar{b}	-0.40	-1.15	-1.69	-1.84	-1.84

in Fig. 3. The only remaining bit corresponds to the expression for the lens equations in terms of the Kalb-Ramond parameter τ and the bulk charge a . This can be achieved by numerically computing the regular part of the integral appearing in the lens equation, which reads, $b_R = 0.9496 - 1.594 a + 0.318 \tau$. Thus finally the lens equation becomes,

$$\Theta(\theta) = -2.1920 - 1.594 a + 0.318 \tau + r_{\text{ph}} \sqrt{\frac{r_{\text{ph}}^3 - 2r_{\text{ph}}^2 - ar_{\text{ph}} - 2\tau}{(r_{\text{ph}}^3 + 2ar_{\text{ph}} + 10\tau)(r_{\text{ph}}^2 - 2r_{\text{ph}} + \tau - a)}} \times \ln \left[\frac{(r_{\text{ph}}^3 + 2ar_{\text{ph}} + 10\tau)(2r_{\text{ph}}^2 + ar_{\text{ph}} + 2\tau)^2}{(r_{\text{ph}}^3 - 2r_{\text{ph}}^2 - ar_{\text{ph}} - 2\tau)(2r_{\text{ph}}^2 + 2ar_{\text{ph}} + 6\tau)(\frac{\theta D_{\text{OL}}}{u_{\text{ph}}} - 1)} \right] \quad (28)$$

Let us now discuss the effect of both the Kalb-Ramond parameter and the bulk effect on the lensing observables. From Table 2 it is clear that an increase in either of τ and a increases the value of the deflection angle and magnification compared to the Schwarzschild one, while the angular separation decreases rapidly. The same behaviour is seen in Fig. 3 as well where it is clear that for a given τ , the deflection angle increases as the bulk charge a increase, while the opposite is seen in the angular separation. Note this this feature distinguishes from the previous model, where the angular separation increases while the magnification decreases. Thus gravitational lensing can act as a test bed for detection of extra dimensions, as the observables behave differently when extra dimensions are present. This might lead to interesting physics as the experimental observations more and more zooms in the near black hole region through future large telescopes.

Table 3: Lensing observables (θ_∞, s, r) and the parameters of the model, $(u_{\text{ph}}, \bar{a}, \bar{b})$ have been estimated numerically. Results for both the Schwarzschild black hole and the black hole in $f(T)$ theory for three possible values of \tilde{q} are presented. In all these calculations, the black hole is taken to be Sgr A^* with mass $M_\bullet = 4.31 \times 10^6 M_\odot$ and distance $D_{\text{OL}} = 8.33$ kpc respectively. Furthermore, the angle θ_∞ and s are expressed in units of micro-arcsecond (μas) and nano-arcsecond (nas) respectively. All the distances are measured with $GM_\bullet/c^2 = 1$ unit.

Observables and Parameters	Schwarzschild	Hole in $f(T)$ gravity		
		$\tilde{q} = 0.2$	$\tilde{q} = 0.5$	$\tilde{q} = 0.8$
θ_∞ (μas)	26.96	26.78	25.78	23.59
s (nas)	33.74	32.98	30.57	36.71
r (mag)	6.82	6.7	6.5	6.29
$u_{\text{ph}}(GM_\bullet/c^2)$	5.20	5.16	4.97	4.55
\bar{a}	1	1.01	1.03	1.12
\bar{b}	-0.40	-0.45	-0.68	-0.98

3.3 Gravitational lensing in $f(T)$ gravity

As the curvature invariants are replaced by Weitzenböck connection one obtains the teleparallel equivalent of general relativity and as a consequence the dynamics is governed by spacetime torsion [60, 61]. The invariant Lagrangian density under general coordinate transformation corresponds to T , which is second order in the torsion tensor. One can extend this framework by considering more general Lagrangian density $f(T)$, which has attracted much attention recently, thanks to its interesting cosmological predictions [62–69]. For an interesting aspect of this in the context of black hole physics, see [70].

Recently, static and spherically symmetric solutions in the context of $f(T)$ gravity have been studied. In this work we will consider one such solution in four dimensions as the $f(T)$ gravity couples with the electromagnetic field. Since we are interested in asymptotically flat solutions, we will neglect the effect of positive cosmological constant and hence the metric elements become [71]

$$f(r) = 1 - \frac{2}{r} + \frac{\tilde{q}^2}{r^2} = g(r) \quad (29)$$

Here, \tilde{q} is the torsion parameter, since the torsion tensor having a single independent component varies as \tilde{q}^2/r^4 [71]. When $\tilde{q} = 0$ one recovers the Schwarzschild solution. We would again like to remind the reader that we are using units in which $GM = 1$. Just as in the previous sections here also we start by computing the photon sphere, which in this case amounts to solving for the algebraic equation $r^2 - 3r + 2\tilde{q}^2 = 0$. This yields the following solution for the photon radius,

$$r_{\text{ph}} = \frac{3}{2} + \frac{1}{2}\sqrt{9 - 8\tilde{q}^2} \quad (30)$$

Given the photon radius r_{ph} , let us now derive the other quantities of interest, which are the impact parameter $u_{\text{ph}} = r_{\text{ph}}/\sqrt{f(r_{\text{ph}})}$ and the \bar{a} and \bar{b} appearing in the lens equation. These three quantities in

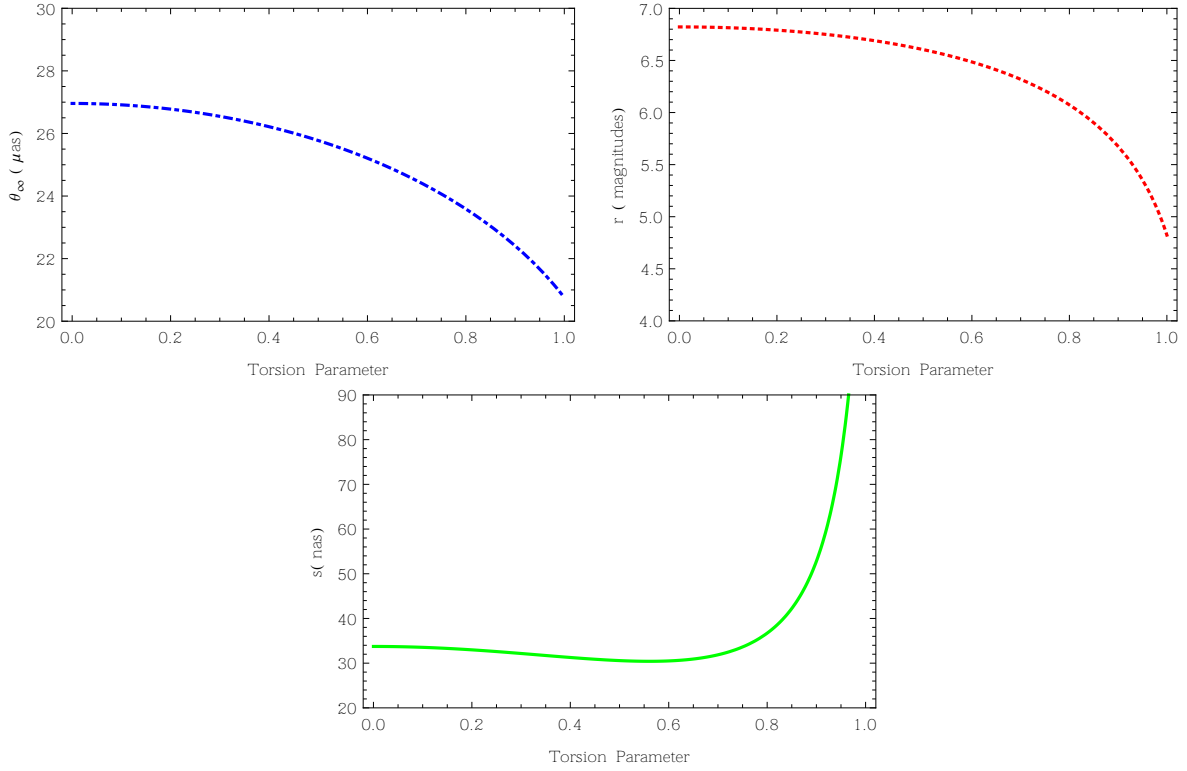


Figure 4: Variation of the three observables, θ_∞ in micro-arcsecond, the magnitude difference r and the angular separation between the outermost and inner images s have been depicted with \tilde{q} . Hence in presence of $f(T)$ gravity in four spacetime dimensions with the increment of the torsion parameter, the corresponding deflection angle and magnitude difference decreases, while the angular separation initially decreases but then exhibits an opposite effect. See text for discussions.

this particular case evaluates to,

$$u_{\text{ph}} = \frac{r_{\text{ph}}^2}{\sqrt{r_{\text{ph}}^2 - 2r_{\text{ph}} + \tilde{q}^2}} \quad (31)$$

$$\bar{a} = \left[1 - \frac{2\tilde{q}^2}{r_{\text{ph}}^2} \right]^{-1/2} \quad (32)$$

$$\bar{b} = -\pi + b_R + \bar{a} \ln \left(\frac{2(r_{\text{ph}}^2 - 2\tilde{q}^2) \left[\frac{2r_{\text{ph}} - \tilde{q}^2}{2r_{\text{ph}} - 2\tilde{q}^2} \right]^2}{r_{\text{ph}}^2 - 2r_{\text{ph}} + \tilde{q}^2} \right) \quad (33)$$

Given these three one can easily estimate numerically the lensing observables, which are presented in [Table 3](#) for three different values of the torsion parameter \tilde{q} using the supermassive black hole Sgr A^* in our galaxy as the gravitational lens. For convenience the corresponding values for $\tilde{q} = 0$, i.e., for Schwarzschild spacetime are also depicted. Further variation of the three observables with \tilde{q} is also illustrated in [Fig. 4](#).

In order to determine the lens equation in this particular scenario one first have to expand the regular part of the integral in the lens equation to leading order in \tilde{q} to yield, $b_R \simeq 0.9496 - 1.5939 \tilde{q}^2$. Thus the lens equation becomes,

$$\Theta(\theta) = -2.192 - 1.5939 \tilde{q}^2 + \left[1 - \frac{2\tilde{q}^2}{r_{\text{ph}}^2} \right]^{-1/2} \ln \left(\frac{2u_{\text{ph}} (r_{\text{ph}}^2 - 2\tilde{q}^2) \left[\frac{2r_{\text{ph}} - \tilde{q}^2}{2r_{\text{ph}} - 2\tilde{q}^2} \right]^2}{(r_{\text{ph}}^2 - 2r_{\text{ph}} + \tilde{q}^2) (\theta D_{\text{OL}} - u_{\text{ph}})} \right) \quad (34)$$

To understand the possible effect of the torsion parameter we consider both [Table 3](#) and [Fig. 4](#) respectively. From the table it is clear that the deflection angle and magnification decreases as \tilde{q} increases, remaining always smaller compared to the Schwarzschild value. Note that this is exactly *opposite* compared to the previous scenarios. On the other hand the angular separation initially shows value small compared to Schwarzschild, but for large enough values of \tilde{q} it increases. Similar features can be visualized through [Fig. 4](#) as well. Again, with increase in resolution, future telescopes will be able to resolve the photon sphere surrounding the black hole. The particular shape one visualizes will depend on the strong gravitational lensing and hence the observables discussed here can have important significance.

4 Concluding Remarks

We have discussed the strong gravitational lensing in the context of both extra dimensions and Kalb-Ramond field. Specifically, we have discussed three situations — (a) Kalb-Ramond field in four spacetime dimensions, (b) Kalb-Ramond field in higher dimensions and its effect on four dimensional brane inherited from the bulk and (c) possible effects of $f(T)$ gravity. In all the three situations we have provided explicit expressions for the three theoretical constructs u_{ph} , \bar{a} and \bar{b} respectively. Using these we have numerically estimated the three observables (θ_∞, s, r) as well as have presented them graphically. To understand possible discord and unity we have presented collectively the behaviour of the observables in these three scenarios in [Table 4](#).

It is clear that all the three scenarios are different in one aspect or another. The deflection angle θ_∞ increases for the Kalb-Ramond field in four and higher dimensions but decreases for $f(T)$ gravity. On

Table 4: A comparison between the three scenarios

Scenario under consideration	Behaviour of deflection (θ_∞)	Behaviour of separation (s)	Behaviour of magnification (r)
Kalb-Ramond field in four dimensions	Increases	Increases	Decreases
Kalb-Ramond field in higher dimensions	Increases	Decreases	Increases
$f(T)$ gravity	Decreases	Initially decreases then increases	Decreases

the other hand, the magnification decreases for Kalb-Ramond field in four dimensions but increases in higher dimensions, while it increases for $f(T)$ gravity. The angular separation shows an opposite effect for Kalb-Ramond field in four and in higher dimensions, while changes from a decreasing to increasing mode in $f(T)$ gravity. Hence the three scenarios offer rich structures and one of the scenario can easily be differentiated from another.

In near future, with either event horizon or square kilometer array operational one can directly measure the photon sphere of the sgr A^* supermassive black hole and hence the observables associated with strong gravitational lensing can be experimentally determined. This will lead to possible constraints on the Kalb-Ramond field parameter as well as spacetime torsion á la strong gravitational lensing. In particular with sufficiently better data one might vote in favour for one particular scenario compared to others. For example, if one observes that the magnification of the image increases compared to the Schwarzschild value, then that will definitely bring forward the scenario of Kalb-Ramond field in higher spacetime dimensions. On the other hand, if the magnification decreases but the deflection angle becomes larger than the Schwarzschild value, then Kalb-Ramond field in four spacetime dimensions would a viable candidate. Hence the study of strong gravitational lensing has the potential to address some of the fundamental questions of the universe, e.g., are there extra spacetime dimensions, why spacetime torsion (or, the Kalb-Ramond field) is missing in our nature, etc.? These would be worthwhile to study in future.

Acknowledgements

A Appendix: Derivation of the lens equation

We will work with the metric ansatz as presented in Eq. (1), which represents the most general static and spherically symmetric spacetime. For the motion of a photon (or a null ray) in this spacetime, the geodesic equations correspond to,

$$\left(\frac{dr}{d\lambda}\right)^2 = \frac{g(r)}{f(r)} \left[E^2 - f(r) \frac{L^2}{r^2} \right] \quad (35)$$

$$\frac{d\phi}{d\lambda} = \frac{L}{r^2} \quad (36)$$

where E and L are the conserved energy and the conserved angular momentum respectively. From these two equations one can eliminate the unknown parameter λ and hence obtain the orbit equation for the null ray, which is given in Eq. (3). A slightly modified version of the orbit equation can be obtained by introducing the impact parameter $b = L/E$ as well as identifying it with a radius r_0 , such that $b = r_0/\sqrt{f(r_0)}$. Integrating this modified orbit equation one obtains the deflection angle as given by Eq. (5). The deflection angle has a divergent part given by,

$$F(x, r_0) = \left[f(r_0) - \frac{r_0^2}{r^2} f(r) \right]^{-1/2} \quad (37)$$

where $x = x(r)$, is an arbitrary function of the radial coordinate r , such that $x(r_0) = 0$. Note that the term within inverse square root vanishes as $r \rightarrow r_0$ and hence $F(x = 0, r_0)$ diverges. Let us now try to expand the term inside square root upto quadratic order in x , which captures the difference $r - r_0$. The first term in the Taylor expansion corresponds to,

$$\alpha = \frac{d}{dx} \left[f(r_0) - \frac{r_0^2}{r^2} f(r) \right] = r_0^2 \left[-\frac{f'(r)}{r^2} + \frac{2f(r)}{r^3} \right] \frac{dr}{dx} \quad (38)$$

Note that when $r = r_{\text{ph}}$, the term vanishes. While the second term yields

$$\begin{aligned} \beta &= \frac{1}{2} \frac{d^2}{dx^2} \left[f(r_0) - \frac{r_0^2}{r^2} f(r) \right] = \frac{1}{2} \frac{dr}{dx} \frac{d\alpha}{dr} \\ &= \frac{r_0^2}{2} \left[\left(\frac{dr}{dx} \right)^2 \left\{ -\frac{f''(r)}{r^2} + \frac{4f'(r)}{r^3} - \frac{6f(r)}{r^4} \right\} + \frac{dr}{dx} \left\{ -\frac{f'(r)}{r^2} + \frac{2f(r)}{r^3} \right\} \frac{d}{dr} \frac{dr}{dx} \right] \end{aligned} \quad (39)$$

On $r = r_{\text{ph}}$, where $r_{\text{ph}} f'(r_{\text{ph}}) = 2f(r_{\text{ph}})$ the above turns out to be,

$$\beta_{\text{ph}} = \frac{r_0^2}{2} \left(\frac{dr}{dx} \right)_{r_{\text{ph}}}^2 \left\{ -\frac{f''(r_{\text{ph}})}{r_{\text{ph}}^2} + \frac{2f(r_{\text{ph}})}{r_{\text{ph}}^4} \right\} \quad (40)$$

Using the above trick one can separate out the integral in Eq. (5) to a divergent and a regular part which yields,

$$I(r_0) = \int_0^{x_\infty} dx \left[\{R(x, r_0)F(x, r_0) - R(0, r_{\text{ph}})F_0(x, r_0)\} + R(0, r_{\text{ph}})F_0(x, r_0) \right] \quad (41)$$

$$= I_R(r_0) + I_D(r_0); \quad F_0(x, r_0) = \frac{1}{\sqrt{\alpha x + \beta x^2}} \quad (42)$$

where, r_{ph} is the radius of photon circular orbit and is a solution of Eq. (2). Given this particular decomposition, the divergent integral $I_D(r_0)$ can be solved explicitly, leading to,

$$\begin{aligned} I_D(r_0) &= \frac{R(0, r_{\text{ph}})}{\sqrt{\beta}} \ln \left[\frac{\alpha + 2\beta + 2\sqrt{\alpha\beta + \beta^2}}{\alpha} \right] \\ &= \frac{2R(0, r_{\text{ph}})}{\sqrt{\beta}} \ln \left[\frac{\sqrt{\beta} + \sqrt{\alpha + \beta}}{\sqrt{\alpha}} \right] \end{aligned} \quad (43)$$

Expanding the above expression around r_{ph} we obtain,

$$\begin{aligned} I_D(r_0) &= -\frac{R(0, r_{\text{ph}})}{\sqrt{\beta_{\text{ph}}}} \ln \left[\alpha_{\text{ph}} + \alpha'_{\text{ph}} r_{\text{ph}} \left(\frac{r_0}{r_{\text{ph}}} - 1 \right) \right] + \frac{R(0, r_{\text{ph}})}{\sqrt{\beta_{\text{ph}}}} \ln(4\beta_{\text{ph}}) + \mathcal{O}(r_0 - r_{\text{ph}}) \\ &= -\frac{R(0, r_{\text{ph}})}{\sqrt{\beta_{\text{ph}}}} \ln \left(\frac{r_0}{r_{\text{ph}}} - 1 \right) - \frac{R(0, r_{\text{ph}})}{\sqrt{\beta_{\text{ph}}}} \ln \left(\frac{\alpha'_{\text{ph}} r_{\text{ph}}}{4\beta_{\text{ph}}} \right) + \mathcal{O}(r_0 - r_{\text{ph}}) \end{aligned} \quad (44)$$

where we have used the result that $r_{\text{ph}} = 0$. From the above discussion it is evident that $\alpha'_{\text{ph}} = (2\beta_{\text{ph}})/(dr/dx)_{\text{ph}}$. Thus finally we obtain,

$$I_D(r_0) = -a \ln \left(\frac{r_0}{r_{\text{ph}}} - 1 \right) + b_D + \mathcal{O}(r_0 - r_{\text{ph}}) \quad (45)$$

where

$$a = \frac{R(0, r_{\text{ph}})}{\sqrt{\beta_{\text{ph}}}}; \quad b_D = -\frac{R(0, r_{\text{ph}})}{\sqrt{\beta_{\text{ph}}}} \ln \left(\frac{r_{\text{ph}}}{2 \left(\frac{dr}{dx} \right)} \right) \quad (46)$$

Let us now introduce another new variable u equivalent to the impact parameter as,

$$u = \frac{r}{\sqrt{f(r)}} \quad (47)$$

such that when Taylor expanded the co-efficients of the first two term at $r = r_{\text{ph}}$ becomes

$$\left(\frac{du}{dr} \right)_{r_{\text{ph}}} = \left[\frac{1}{\sqrt{f}} - \frac{1}{2} \frac{r f'(r)}{f^{3/2}(r)} \right]_{r_{\text{ph}}} = 0 \quad (48)$$

and

$$\frac{1}{2} \left(\frac{d^2 u}{dr^2} \right)_{r_{\text{ph}}} = \frac{1}{2} \left[-\frac{f'(r)}{f^{3/2}(r)} - \frac{r f''(r)}{2 f^{3/2}(r)} + \frac{3 r f'^2(r)}{4 f^{5/2}(r)} \right]_{r_{\text{ph}}} = \frac{1}{4 r_{\text{ph}} f^{3/2}(r_{\text{ph}})} [2f(r_{\text{ph}}) - r_{\text{ph}}^2 f''(r_{\text{ph}})] \quad (49)$$

Thus,

$$u - u_{\text{ph}} = c (r - r_{\text{ph}})^2 \quad (50)$$

where,

$$c = \frac{1}{4 r_{\text{ph}} f^{3/2}(r_{\text{ph}})} [2f(r_{\text{ph}}) - r_{\text{ph}}^2 f''(r_{\text{ph}})] = \frac{r_{\text{ph}}^3 \beta_{\text{ph}}}{2 r_0^2 f^{3/2}(r_{\text{ph}})} \left(\frac{dr}{dx} \right)_{r_{\text{ph}}}^{-2} \quad (51)$$

Hence the divergent integral turns out to be,

$$\begin{aligned} I_D(r_0) &= -a \ln \left(\frac{\sqrt{u_{\text{ph}}} \sqrt{\frac{u_0}{u_{\text{ph}}} - 1}}{r_{\text{ph}} \sqrt{c}} \right) + b_D + \mathcal{O}(r_0 - r_{\text{ph}}) \\ &= -\frac{a}{2} \ln \left(\frac{u_0}{u_{\text{ph}}} - 1 \right) - a \ln \left(\frac{r_{\text{ph}}}{2 \left(\frac{dr}{dx} \right)} \right) - a \ln \left(\frac{\sqrt{u_{\text{ph}}}}{r_{\text{ph}} \sqrt{c}} \right) + \mathcal{O}(r_0 - r_{\text{ph}}) \\ &= -\frac{a}{2} \ln \left(\frac{u_0}{u_{\text{ph}}} - 1 \right) - \frac{a}{2} \ln \left(\frac{u_{\text{ph}}}{4c \left(\frac{dr}{dx} \right)^2} \right) \end{aligned} \quad (52)$$

Substituting for c , we immediately arrived at,

$$\begin{aligned}
I_D(r_0) &= -\frac{a}{2} \ln \left(\frac{u_0}{u_{\text{ph}}} - 1 \right) - \frac{a}{2} \ln \left[\frac{r_{\text{ph}}}{4\sqrt{f(r_{\text{ph}})}} \frac{1}{\left(\frac{dr}{dx}\right)^2} \left(\frac{r_{\text{ph}}^3 \beta_{\text{ph}}}{2r_0^2 f^{3/2}(r_{\text{ph}})} \right)^{-1} \left(\frac{dr}{dx} \right)^2_{r_{\text{ph}}} \right] \\
&= -\frac{a}{2} \ln \left(\frac{u_0}{u_{\text{ph}}} - 1 \right) + \frac{a}{2} \ln \left(\frac{2r_{\text{ph}}^2}{r_0^2} \frac{\beta_{\text{ph}}}{f(r_{\text{ph}})} \right)
\end{aligned} \tag{53}$$

Now if θ is the angle between the image and the lens, one readily obtains the following result for deflection angle in terms of θ as in Eq. (6). The objects present in the Lens equation has the following expressions

$$\bar{a} = \frac{R(0, r_{\text{ph}})}{2\sqrt{\beta_{\text{ph}}}}; \quad \bar{b} = -\pi + b_R + \bar{a} \ln \left(\frac{2\beta_{\text{ph}}}{f(r_{\text{ph}})} \right) \tag{54}$$

where the quantity b_R corresponds to,

$$b_R = I_R(r_{\text{ph}}) = \int_{x_{\text{ph}}}^{x_\infty} dx \{R(x, r_{\text{ph}})F(x, r_{\text{ph}}) - R(0, r_{\text{ph}})F_0(x, r_{\text{ph}})\} \tag{55}$$

These are used in order to obtain Eq. (7), Eq. (8) and Eq. (9).

References

- [1] P. Schneider, J. Ehlers, and E. E. Falco, *Gravitational Lenses*. Springer-Verlag, 1992.
- [2] S. Liebes, “Gravitational Lenses,” *Phys. Rev.* **133** (1964) B835–B844.
- [3] S. Refsdal and J. Surdej, “Gravitational lenses,” *Rept. Prog. Phys.* **57** (1994) 117–186.
- [4] K. S. Virbhadra and G. F. R. Ellis, “Schwarzschild black hole lensing,” *Phys. Rev.* **D62** (2000) 084003, [arXiv:astro-ph/9904193](#) [astro-ph].
- [5] S. Frittelli, T. P. Kling, and E. T. Newman, “Space-time perspective of Schwarzschild lensing,” *Phys. Rev.* **D61** (2000) 064021, [arXiv:gr-qc/0001037](#) [gr-qc].
- [6] V. Bozza, S. Capozziello, G. Iovane, and G. Scarpetta, “Strong field limit of black hole gravitational lensing,” *Gen. Rel. Grav.* **33** (2001) 1535–1548, [arXiv:gr-qc/0102068](#) [gr-qc].
- [7] V. Bozza, “Gravitational lensing in the strong field limit,” *Phys. Rev.* **D66** (2002) 103001, [arXiv:gr-qc/0208075](#) [gr-qc].
- [8] E. F. Eiroa, G. E. Romero, and D. F. Torres, “Reissner-Nordstrom black hole lensing,” *Phys. Rev.* **D66** (2002) 024010, [arXiv:gr-qc/0203049](#) [gr-qc].
- [9] V. Bozza, F. De Luca, and G. Scarpetta, “Kerr black hole lensing for generic observers in the strong deflection limit,” *Phys. Rev.* **D74** (2006) 063001, [arXiv:gr-qc/0604093](#) [gr-qc].
- [10] G. V. Kraniotis, “Gravitational lensing and frame dragging of light in the Kerr-Newman and the Kerr-Newman-(anti) de Sitter black hole spacetimes,” *Gen. Rel. Grav.* **46** no. 11, (2014) 1818, [arXiv:1401.7118](#) [gr-qc].

- [11] E. F. Eiroa, “Gravitational lensing by Einstein-Born-Infeld black holes,” *Phys. Rev.* **D73** (2006) 043002, [arXiv:gr-qc/0511065 \[gr-qc\]](#).
- [12] S.-b. Chen and J.-l. Jing, “Strong field gravitational lensing in the deformed Horava-Lifshitz black hole,” *Phys. Rev.* **D80** (2009) 024036, [arXiv:0905.2055 \[gr-qc\]](#).
- [13] R. Whisker, “Strong gravitational lensing by braneworld black holes,” *Phys. Rev.* **D71** (2005) 064004, [arXiv:astro-ph/0411786 \[astro-ph\]](#).
- [14] A. Bhadra, “Gravitational lensing by a charged black hole of string theory,” *Phys. Rev.* **D67** (2003) 103009, [arXiv:gr-qc/0306016 \[gr-qc\]](#).
- [15] T. Ghosh and S. Sengupta, “Strong gravitational lensing across dilaton anti-de Sitter black hole,” *Phys. Rev.* **D81** (2010) 044013, [arXiv:1001.5129 \[gr-qc\]](#).
- [16] N. Mukherjee and A. S. Majumdar, “Particle motion and gravitational lensing in the metric of a dilaton black hole in a de Sitter universe,” *Gen. Rel. Grav.* **39** (2007) 583–600, [arXiv:astro-ph/0605224 \[astro-ph\]](#).
- [17] E. F. Eiroa and C. M. Sendra, “Regular phantom black hole gravitational lensing,” *Phys. Rev.* **D88** no. 10, (2013) 103007, [arXiv:1308.5959 \[gr-qc\]](#).
- [18] G. N. Gyulchev and I. Z. Stefanov, “Gravitational Lensing by Phantom Black holes,” *Phys. Rev.* **D87** no. 6, (2013) 063005, [arXiv:1211.3458 \[gr-qc\]](#).
- [19] S.-S. Zhao and Y. Xie, “Strong field gravitational lensing by a charged Galileon black hole,” *JCAP* **1607** no. 07, (2016) 007, [arXiv:1603.00637 \[gr-qc\]](#).
- [20] K. K. Nandi, Y.-Z. Zhang, and A. V. Zakharov, “Gravitational lensing by wormholes,” *Phys. Rev.* **D74** (2006) 024020, [arXiv:gr-qc/0602062 \[gr-qc\]](#).
- [21] S. W. Wei, Y. X. Liu, and C. E. Fu, “Null Geodesics and Gravitational Lensing in a Nonsingular Spacetime,” *Adv. High Energy Phys.* **2015** (2015) 454217, [arXiv:1510.02560 \[gr-qc\]](#).
- [22] S. Sahu, K. Lochan, and D. Narasimha, “Gravitational lensing by self-dual black holes in loop quantum gravity,” *Phys. Rev.* **D91** (2015) 063001, [arXiv:1502.05619 \[gr-qc\]](#).
- [23] K. S. Virbhadra and G. F. R. Ellis, “Gravitational lensing by naked singularities,” *Phys. Rev.* **D65** (2002) 103004.
- [24] S. Sahu, M. Patil, D. Narasimha, and P. S. Joshi, “Can strong gravitational lensing distinguish naked singularities from black holes?,” *Phys. Rev.* **D86** (2012) 063010, [arXiv:1206.3077 \[gr-qc\]](#).
- [25] P. Amore, M. Cervantes, A. De Pace, and F. M. Fernandez, “Gravitational lensing from compact bodies: Analytical results for strong and weak deflection limits,” *Phys. Rev.* **D75** (2007) 083005, [arXiv:gr-qc/0610153 \[gr-qc\]](#).
- [26] V. Bozza, “Gravitational Lensing by Black Holes,” *Gen. Rel. Grav.* **42** (2010) 2269–2300, [arXiv:0911.2187 \[gr-qc\]](#).
- [27] B. Raffaelli, “Strong gravitational lensing and black hole quasinormal modes: Towards a semiclassical unified description,” *Gen. Rel. Grav.* **48** no. 2, (2016) 16, [arXiv:1412.7333 \[gr-qc\]](#).

- [28] **Perimeter Institute for Theoretical Physics** Collaboration, A. E. Broderick, T. Johannsen, A. Loeb, and D. Psaltis, “Testing the No-Hair Theorem with Event Horizon Telescope Observations of Sagittarius A*,” *Astrophys. J.* **784** (2014) 7, [arXiv:1311.5564 \[astro-ph.HE\]](#).
- [29] V. Bozza and L. Mancini, “Gravitational lensing by black holes: A Comprehensive treatment and the case of the star S2,” *Astrophys. J.* **611** (2004) 1045–1053, [arXiv:astro-ph/0404526 \[astro-ph\]](#).
- [30] A. A. Abdujabbarov, L. Rezzolla, and B. J. Ahmedov, “A coordinate-independent characterization of a black hole shadow,” *Mon. Not. Roy. Astron. Soc.* **454** no. 3, (2015) 2423–2435, [arXiv:1503.09054 \[gr-qc\]](#).
- [31] H. Falcke and S. B. Markoff, “Toward the event horizon—the supermassive black hole in the Galactic Center,” *Class. Quant. Grav.* **30** (2013) 244003, [arXiv:1311.1841 \[astro-ph.HE\]](#).
- [32] V. Bozza and L. Mancini, “Observing gravitational lensing effects by Sgr A* with GRAVITY,” *Astrophys. J.* **753** (2012) 56, [arXiv:1204.2103 \[astro-ph.GA\]](#).
- [33] A. Y. Bin-Nun, “Strong Gravitational Lensing by Sgr A*,” *Class. Quant. Grav.* **28** (2011) 114003, [arXiv:1011.5848 \[gr-qc\]](#).
- [34] M. B. Green, J. H. Schwarz, and E. Witten, *Superstring Theory. Vol. 2: Loop Amplitudes, Anomalies and Phenomenology*. 1988. <http://www.cambridge.org/us/academic/subjects/physics/theoretical-physics-and-mathematical-physics/superstring-theory-volume-2>.
- [35] S. Chakraborty and S. SenGupta, “Spherically symmetric brane spacetime with bulk $f(\mathcal{R})$ gravity,” *Eur.Phys.J.* **C75** no. 1, (2015) 11, [arXiv:1409.4115 \[gr-qc\]](#).
- [36] S. Chakraborty and S. SenGupta, “Effective gravitational field equations on m -brane embedded in n -dimensional bulk of Einstein and $f(\mathcal{R})$ gravity,” *Eur. Phys. J.* **C75** no. 11, (2015) 538, [arXiv:1504.07519 \[gr-qc\]](#).
- [37] S. Chakraborty and S. SenGupta, “Spherically symmetric brane in a bulk of $f(\mathcal{R})$ and Gauss-Bonnet Gravity,” *Class. Quant. Grav.* **33** no. 22, (2016) 225001, [arXiv:1510.01953 \[gr-qc\]](#).
- [38] S. Chakraborty and S. SenGupta, “Solving higher curvature gravity theories,” *Eur. Phys. J.* **C76** no. 10, (2016) 552, [arXiv:1604.05301 \[gr-qc\]](#).
- [39] P. S. Howe and G. Papadopoulos, “Twistor spaces for HKT manifolds,” *Phys. Lett.* **B379** (1996) 80–86, [arXiv:hep-th/9602108 \[hep-th\]](#).
- [40] S. Kar, P. Majumdar, S. SenGupta, and S. Sur, “Cosmic optical activity from an inhomogeneous Kalb-Ramond field,” *Class. Quant. Grav.* **19** (2002) 677–688, [arXiv:hep-th/0109135 \[hep-th\]](#).
- [41] P. S. Letelier, “Spinning strings as torsion line space-time defects,” *Class. Quant. Grav.* **12** (1995) 471–478.
- [42] J. Ellis, N. E. Mavromatos, and S. Sarkar, “Environmental CPT Violation in an Expanding Universe in String Theory,” *Phys. Lett.* **B725** (2013) 407–411, [arXiv:1304.5433 \[gr-qc\]](#).
- [43] D. Maity, P. Majumdar, and S. SenGupta, “Parity violating Kalb-Ramond-Maxwell interactions and CMB anisotropy in a brane world,” *JCAP* **0406** (2004) 005, [arXiv:hep-th/0401218 \[hep-th\]](#).

- [44] P. Majumdar and S. SenGupta, “Parity violating gravitational coupling of electromagnetic fields,” *Class. Quant. Grav.* **16** (1999) L89–L94, [arXiv:gr-qc/9906027 \[gr-qc\]](#).
- [45] R. Myrzakulov, “Accelerating universe from F(T) gravity,” *Eur. Phys. J.* **C71** (2011) 1752, [arXiv:1006.1120 \[gr-qc\]](#).
- [46] S.-H. Chen, J. B. Dent, S. Dutta, and E. N. Saridakis, “Cosmological perturbations in f(T) gravity,” *Phys. Rev.* **D83** (2011) 023508, [arXiv:1008.1250 \[astro-ph.CO\]](#).
- [47] J. B. Dent, S. Dutta, and E. N. Saridakis, “f(T) gravity mimicking dynamical dark energy. Background and perturbation analysis,” *JCAP* **1101** (2011) 009, [arXiv:1010.2215 \[astro-ph.CO\]](#).
- [48] K. Bamba, C.-Q. Geng, C.-C. Lee, and L.-W. Luo, “Equation of state for dark energy in $f(T)$ gravity,” *JCAP* **1101** (2011) 021, [arXiv:1011.0508 \[astro-ph.CO\]](#).
- [49] Y. Zhang, H. Li, Y. Gong, and Z.-H. Zhu, “Notes on $f(T)$ Theories,” *JCAP* **1107** (2011) 015, [arXiv:1103.0719 \[astro-ph.CO\]](#).
- [50] S. Chakraborty, “An alternative f(R, T) gravity theory and the dark energy problem,” *Gen. Rel. Grav.* **45** (2013) 2039–2052, [arXiv:1212.3050 \[physics.gen-ph\]](#).
- [51] R.-J. Yang, “Conformal transformation in $f(T)$ theories,” *Europhys. Lett.* **93** (2011) 60001, [arXiv:1010.1376 \[gr-qc\]](#).
- [52] S. Bhattacharya and S. Chakraborty, “Solar system constraints on some Horndeski gravity theories,” [arXiv:1607.03693 \[gr-qc\]](#).
- [53] S. Chakraborty and S. Chakraborty, “Trajectory around a spherically symmetric non-rotating black hole,” *Can.J.Phys.* **89** (2011) 689–695, [arXiv:1109.0676 \[gr-qc\]](#).
- [54] S. Chakraborty, “Equilibrium configuration of perfect fluid orbiting around black holes in some classes of alternative gravity theories,” *Class.Quant.Grav.* **32** no. 7, (2015) 075007, [arXiv:1406.0417 \[gr-qc\]](#).
- [55] S. Chakraborty, “Aspects of Neutrino Oscillation in Alternative Gravity Theories,” *JCAP* **1510** no. 10, (2015) 019, [arXiv:1506.02647 \[gr-qc\]](#).
- [56] S. Kar, S. SenGupta, and S. Sur, “Static spherisymmetric solutions, gravitational lensing and perihelion precession in Einstein-Kalb-Ramond theory,” *Phys. Rev.* **D67** (2003) 044005, [arXiv:hep-th/0210176 \[hep-th\]](#).
- [57] S. SenGupta and S. Sur, “Spherically symmetric solutions of gravitational field equations in Kalb-Ramond background,” *Phys. Lett.* **B521** (2001) 350–356, [arXiv:gr-qc/0102095 \[gr-qc\]](#).
- [58] S. Chakraborty and S. SenGupta, “Solutions on a brane in a bulk spacetime with Kalb-Ramond field,” *Annals Phys.* **367** (2016) 258–279, [arXiv:1412.7783 \[gr-qc\]](#).
- [59] N. Dadhich, R. Maartens, P. Papadopoulos, and V. Rezanian, “Black holes on the brane,” *Phys.Lett.* **B487** (2000) 1–6, [arXiv:hep-th/0003061 \[hep-th\]](#).
- [60] R. Ferraro and F. Fiorini, “Modified teleparallel gravity: Inflation without inflaton,” *Phys. Rev.* **D75** (2007) 084031, [arXiv:gr-qc/0610067 \[gr-qc\]](#).

- [61] R. Ferraro and F. Fiorini, “On Born-Infeld Gravity in Weitzenbock spacetime,” *Phys. Rev.* **D78** (2008) 124019, [arXiv:0812.1981 \[gr-qc\]](#).
- [62] M. Hamani Daouda, M. E. Rodrigues, and M. J. S. Houndjo, “Static Anisotropic Solutions in $f(T)$ Theory,” *Eur. Phys. J.* **C72** (2012) 1890, [arXiv:1109.0528 \[physics.gen-ph\]](#).
- [63] S. Capozziello, G. Lambiase, and C. Stornaiolo, “Geometric classification of the torsion tensor in space-time,” *Annalen Phys.* **10** (2001) 713–727, [arXiv:gr-qc/0101038 \[gr-qc\]](#).
- [64] S. Capozziello and M. Francaviglia, “Extended Theories of Gravity and their Cosmological and Astrophysical Applications,” *Gen. Rel. Grav.* **40** (2008) 357–420, [arXiv:0706.1146 \[astro-ph\]](#).
- [65] R. Myrzakulov, “FRW Cosmology in $F(R,T)$ gravity,” *Eur. Phys. J.* **C72** (2012) 2203, [arXiv:1207.1039 \[gr-qc\]](#).
- [66] M. I. Wanas and H. A. Hassan, “Torsion and Problems of Standard Cosmology,” [arXiv:1209.6218 \[gr-qc\]](#).
- [67] V. Faraoni and S. Capozziello, *Beyond Einstein Gravity*, vol. 170. 170 of *Fundamental Theories of Physics*. Springer, Dordrecht, 2011. <http://www.springerlink.com/content/hl1805/#section=801705&page=1>.
- [68] R. Ferraro and F. Fiorini, “Non trivial frames for $f(T)$ theories of gravity and beyond,” *Phys. Lett.* **B702** (2011) 75–80, [arXiv:1103.0824 \[gr-qc\]](#).
- [69] R.-X. Miao, M. Li, and Y.-G. Miao, “Violation of the first law of black hole thermodynamics in $f(T)$ gravity,” *JCAP* **1111** (2011) 033, [arXiv:1107.0515 \[hep-th\]](#).
- [70] K. Lochan and S. Chakraborty, “Discrete quantum spectrum of black holes,” *Phys. Lett.* **B755** (2016) 37–42, [arXiv:1509.09010 \[gr-qc\]](#).
- [71] S. Capozziello, P. A. Gonzalez, E. N. Saridakis, and Y. Vasquez, “Exact charged black-hole solutions in D-dimensional $f(T)$ gravity: torsion vs curvature analysis,” *JHEP* **02** (2013) 039, [arXiv:1210.1098 \[hep-th\]](#).